ANALYSIS AND UNDERSTANDING OF HEAT TREATMENT OF L-PBF TITANIUM PRODUCTS

Philip Simões Carvalho
philipcarvalho@tecnico.ulisboa.pt

Instituto Superior Técnico, Universidade de Lisboa, Portugal

September 2021

Abstract

3D printing has brought on an endless number of possibilities when it comes to producing parts made of metal due to the complex geometries and the wide variety of different materials that can be used to produce them. However, while very useful, printing through Laser Powder Bed Fusion still results in the production of parts with many crippling flaws like melt pool discontinuities and entrapped vaporized material that have a significant impact in their mechanical properties. To solve these issues, a number of different post-treatment processes can be applied to the produced parts, namely heat treatments.

This work strived to determine how regular heat treating parameters affect the final mechanical properties of titanium alloy L-PBF produced parts. A total of 86 testing coupons were produced, 81 of which were submitted to heat treatments with several different combinations of sitting temperatures, sitting times and cooling rates. The Design of Experiments was created using a statistical software. After, some mechanical properties of the 84 coupons were obtained through tensile and hardness testing. Lastly, the optimal parameters for enhancing the desired properties were obtained through an analysis performed using the same statistical program.

It was concluded that replicating the same results in an L-PBF print is complicated when there isn't a tight control over all variables like printing parameters or the quality of the powder. Only one set of parameters can be used for each print type as even the slightest difference, like changing the orientation of the components, can render the parameters non-optimal. The higher the resting temperature in the heat treatments is, the higher the hardness.

Keywords: Titanium, L-PBF, Mechanical Properties, Heat Treatment

1. Introduction

Ensuring the best possible results when producing titanium alloy parts through Laser Powder Bed Fusion is of utmost importance as many parts will be used in applications that require them not to fail under any circumstance. It is known that putting these parts through certain extreme temperature variations can alter their mechanical properties either through the elimination of defects or through the change in microstructure.

Understanding how these heat treatments affect these parts will provide the knowledge needed to efficiently treat them after production in order to obtain the desired mechanical properties.

Additive manufacturing consists producing parts layer by layer. As opposed to traditional ways of manufacturing, also known as subtractive manufacturing, it usually allows for more complex geometries with less steps at the cost of higher prices and longer manufacturing times. It can use a wide variety of materials like metals, plastics or resins that, in turn, can come in many forms like powder or wire.

While useful, there is still a long way to go regarding the production of parts that are ready to be used as-built. The downsides of this process make it so only the industries that can benefit the most from it can use it, like the aerospace and the medical industries. With their tight tolerances and requirement for complex and custom parts, the need to improve the overall quality is clear. This can be done through two approaches: improving and perfecting the build parameters of the part or subjecting the part to post-processing like surface finishing or heat treating.

There are already a wide variety of known heat treating methods that yield specific results in specific materials. However, these are more established for parts produced through traditional manufacturing. Parts produced through additive manufacturing acquire specific defects that require different types heat treatments. While some studies have

been done in this field, it is still open to more research.

2. Experimental Methods

The experimental approach consists of producing Ti-6Al-4V testing coupons through Laser - Powder Bed Fusion, heat treating them at different parameters and then testing them and analyzing the results.

According to the DOE, groups of 3 testing coupons were subjected to heat treatments with different combinations of parameters. These heat treatments vary according to the sitting temperature, the sitting time and the cooling rate and will all occur in an inert atmosphere. Each of these parameters have 3 different values each, and would result in a total of 27 different sets of values.

However, after a miscommunication with the company performing the heat treatments, it was revealed that one of the cooling methods was wrongfully used. One third of the coupons were oil quenched as opposed to air cooled. As this was thought to not yield the desired results for the subsequent analysis, it was agreed that two thirds of the affected coupons (18 out of the 27) would be reheated with the same established parameters and cooled with the originally planned method, air cooling. This resulted in 36 different sets of parameters.

Following the treatments, they were subjected to mechanical testing, namely hardness tests and tensile testing. Aside from these heat treated coupons, 5 more as-built coupons were subjected to the same mechanical tests for comparison. This brought the total testing coupons to 86.

2.1. Material

The material used was Ti-6Al-4V Grade 23 Powder from AP&C produced by plasma atomization, with a density of 2.52 g/cm^3 and a particle size ranging from 10 to 45 μm. The material composition of the used powder can be found in table 1.

Material	Amount [Wt. %]
Aluminum, Al	6.44
Vanadium, V	3.91
Iron, Fe	0.20
Oxygen, O	0.13
Carbon, C	0.01
Nitrogen, N	0.01
Hydrogen, H	0.002
Yttrium, Y	<0.001
Other Each	<0.08
Other Total	<0.20
Ti	Balance

Table 1: Composition of the powder used to produce the testing coupons according to the manufacturer.

It's relevant to point out that the normal density value for this material is of about 4.41 g/cm^3 [1]; there is a very large gap in the density value of the powder provided and the theoretical one.

2.2. Printing

The machine and computer program used to print the parts were the RenAM 500PM and QuantAM from Renishaw. The coupons were laid out vertically in a grid of 8 rows and 11 columns adding to a total of 88, 86 of which were used for this thesis. The coupons to be printed are the standard sheet-type specimens according to standard ASTM E8 with a thickness of 4 mm. As for the printing parameters, which are shown in table 2.2, these were chosen based on a previous master's dissertation [2] performed to optimize the printing of parts made from the same material in the same printing machine.

Parameter	Value
Laser Diameter [μm]	75
Laser Frequency [kHz]	100
Power [W]	200
Layer Thickness [μm]	60
Total Layers	1666
Scanning Strategy	Stripe
Point Distance [μm]	60
Exposure Time [μs]	70
Angle Between Layers [º]	67
Hatch Spacing [μm]	95
Volumetric Energy Density [J/mm^3]	40.935

Table 2: List of the main printing parameters.

2.3. DOE

In table 3, the DOE for the production of the aforementioned testing coupons is shown presenting the specific values for the parameters of the heat treatments. Evaluating the behaviour of the Ti-6Al-4V near the β-transus (1000 ºC) was a priority, so temperatures immediately above and below it were chosen (950 ºC and 1100 ºC). The remaining values were chosen as they seemed the most commonly used in the literature and the most relevant to develop on.

As previously explained, the original DOE consisted solely of 3 different levels for each parameter leading to 27 different combinations evenly spread through 81 coupons. However, after mistakenly oil quenching the coupons that were supposed to be air cooled (27 coupons), it was decided to keep one third of them as they were (9) and to repeat the originally planned heat treatment for the rest (18). This means that, in the end, there are 36 different parameter combinations: 18 of those represented in 3 coupons (the water quenched and furnace cooled),

Factor	Name	Units	Low Level	Middle Level	High Level
A	Resting Temperature	ºC	800	950	1100
B	Resting Time	hours	0.5	3	5
C	Cooling Rate	-	Furnace Cooling	Air Cooling (after oil quenched)	Water/Oil Quenching

Table 3: Design of Experiments.

9 in 2 coupons (oil quenched then air cooled) and 9 in 1 coupon (oil quenched).

2.4. **Equipment**

The testing coupons were designed according to the ASTM E8 standard using the software Magics at IMR. This software was used for its features, among which are the ability to prepare the .STL files for use in AM by accounting for support structures.

The 3D printer used for this thesis was the RenAM 500M developed by Renishaw. It sports a 500 W ytterbium fiber laser and a 250 mm x 250 mm x 350 mm build volume. It also contains features such as on board sieving and powder recirculation as well as a dual SafeChange filter that automatically senses and redirects recirculation gas to maintain optimal performance and chamber cleanliness. This 3D printer works in tandem with the QuantAM software provided by the same company which allows for the preparation of parts for 3D printing.

The heat treatments for this thesis were done in collaboration with the Material Services branch of the company Thyssenkrupp in Marinha Grande, Portugal. The heat treatments were done in a vacuum.

The polishing and grinding of the testing coupons were done using a Struers LaboPol-30 for wider sides and a Multi 395 Dremel with a grinding tip for the narrow sides. While polishing, the discs were rotating at 500 rpm and the coupons were actively cooled through a stream of water.

The tensile testing was performed using an Instron 4507 with a 200 kN load cell and a Static Axial Clip-On Instron Extensometer. A custom part was designed and 3D-printed to be used with the extensometer because the base model was too large to be used with the coupons.

The microhardness testing was done using a Struers Duramin with a Vickers indenter tip.

2.5. **Methodology**

The tensile tests were performed using a 2 kN/min load which changed to a crosshead speed of 5 mm/min after the grips moved 0.12 mm apart. The obtained results were the Young's Modulus, the yield strength (obtained with the 0.2 % rule), the ultimate tensile strength, the maximum elongation and the fracture strength. For the hardness tests, 5 indentations were performed on the polished surface of each sample with a load of 19.614 N for a duration of 20 seconds. Only one coupon from each combination of parameters was tested plus as-built coupons P4 and P5.

3. Results and Discussion

The main focus of this dissertation was to investigate and optimize the heat treatment process of Ti-6Al-4V components produced by an L-PBF machine. Since this is being done in the context of medical devices, ideally, the components would have high strength, moderate hardness and ductility. This dissertation was also developed as the continuation of another dissertation [2] that studied the effects of the printing parameters on the mechanical properties of Ti-6Al-4V components. The coupons used for this dissertation were printed using the best parameter combination found in that dissertation. The DOE that had been originally developed for the analysis of this dissertation will not be used to analyse the results due to their inconsistency with the literature, which will be further discussed in this section. Originally, there had been plans to perform tensile tests on all of the produced coupons. However, due to time constraints and slippage of the coupons during the tensile testing, only 14 of the heat treated samples were successfully tested.

3.1. **As-Built Coupons**

As for the results, these were not expected. In all 5 tests the coupons averaged a fracture strength of 868.53 MPa never having reached the yield point. The maximum values for elongation fell just below 1%. The main source for comparison is the aforementioned dissertation [2] where, regardless of the parameters used for the print, the majority of coupons reached the plastic deformation region with a yield strength in the 1030 to 1120 MPa range, an elongation ranging from 2 to 5 % and a UTS of at least 1150 MPa. In the literature, Liu et al. [3] compiled a list of numerous tensile tests performed in various different studies to Ti-6Al-4V coupons with different build orientations and print parameters. The UTS results varied between 1000 and 1450 MPa, yield strengths between 850 and 1300 MPa and elongations between 1.4 and 11.3 %.

This data serves to show how inconsistent the mechanical properties of L-PBF produced components can be and how dependent they are of the printing parameters used [4]. Even though this print was performed using the optimized printing parameters obtained by Ropio in [2], the fact that the coupons were laid out vertically as opposed to horizontally

Sample No.	E [GPa]	UTS [MPa]	σ_y [MPa]	Strain [%]	σ_f [MPa]
P1		765.11	-		765.11
P2		961.38	-		961.38
P3		849.33	-		849.33
P4	119.34	900.97	-	0.84	900.97
P5	95.47	865.86	-	0.90	865.86

Table 4: Results obtained from tensile testing done to the non heat treated coupons.

might have been enough to cause the defects responsible for this mechanical behaviour [5, 6]. Even if all the printing parameters are maintained, changing the orientation of the component on the build plate is known to be enough to cause noticeable differences in mechanical performance [7]. In all of these studies mentioned previously, the non heat treated coupons still reached the plastic deformation region regardless of being machined or not. This evidences the fact that there is something inherently wrong with the machined as-built coupons used as the baseline. It is worth noting that even some articles refer the need to re-print some samples due to poor mechanical performance as exemplified by Vilaro et al. in their article [7].

Figure 1: Fracture surface of coupon P5. The photo was taken with a cellphone through a microscope.

In figure 1 the fracture surface is represented. Although the quality isn't the best, porosity is still very visible throughout the surface. The round pores are too large to be identified as gas pores (200 μm) but some lack of fusion can be identified in the right side of the fracture, where bright pores with irregular shapes can be seen. In this image it's not very clear, but with the naked eye a more ductile fracture can be seen from the border up to a depth of 0.5 mm, the rest being fragile.

The L-PBF production method is known to produce components with many flaws and defects. The mechanical properties were definitely improved by the heat treatments, in certain cases. This allows for narrowing down which of these defects might be causing the problems. The defects that are most likely to be corrected during the heat treatment processes are the lack of fusion, the residual stresses and the poor microstructure. This means that all other defects (anisotropy, gas pores, balling, hot tears and fish scales) will still be present in the final parts inevitably affecting the mechanical performance. Unfortunately, due to lack of time, a more in-depth investigation exploring the full extent of these defects is not possible.

3.2. Heat Treated Coupons

In this section, the tensile results of the heat treated coupons will be presented, discussed and compared to the as-built coupons from the previous section and the Ropio's dissertation in order to determine how effective they were at improving their properties.

3.2.1 Sitting Temperature - 800 °C

Looking at the coupons heat treated at 800 °C, they all reach values of UTS between 1130 and 1200 MPa. However, those that were treated for 0.5 h present strain values up to 6 %. The ones treated for 3 h reached 8.22 % (furnace cooled) and 9.61 % (water quenched). Interestingly, the specimen that has the highest fracture strain also has the lowest yield stress of coupons that reached the plastic region. The yield stresses covered a wide range from 850 to 1100 MPa. Just like the yield stresses, the elasticity moduli values covered a wide range (90-127 GPa), which is generally not expected and is certainly a result of the defects still present in the specimens.

It seems like the temperature at which the coupons were treated was the main impacting factor of the UTS as it was the only common factor among the parts. After that, the resting time played the major role in affecting the elongation values as they increased for higher times. This is consistent with the fact that the low ductility microstructure found in as-built parts, α'-phase martensite, starts to decompose into more favorable $\alpha + \beta$ phases at around 800 °C. [8] The longer siting times allow for a greater amount of the previous microstructure to be transformed, and thus improve its ductile properties while maintaining the UTS. At sub-transus temperatures, the cooling rate is expected to be the factor with less influence in the final properties.

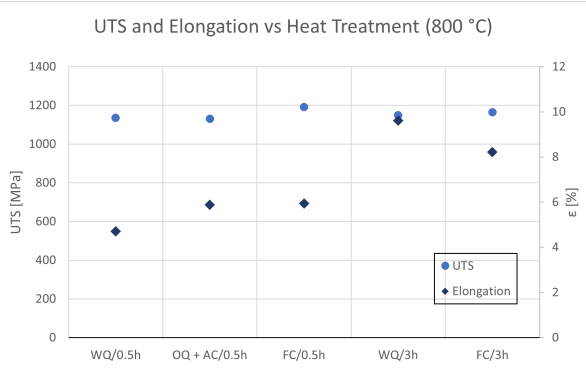

Figure 2: Graphical representation of the UTS and the elongation according to the applied heat treatment, more specifically, at the sitting temperature of 800 °C.

3.2.2 Sitting Temperature - 950 °C

At this temperature there's a general decline of the mechanical properties when compared to the coupons treated at 800 °C. As seen in figure 3, half of the 4 coupons didn't reach the phase of plastic deformation. Those that did, reached UTS values of 1100 and 1000 MPa and yield stresses of 911 and 930 MPa. However, the strain values were very low, at about 2.5 %.

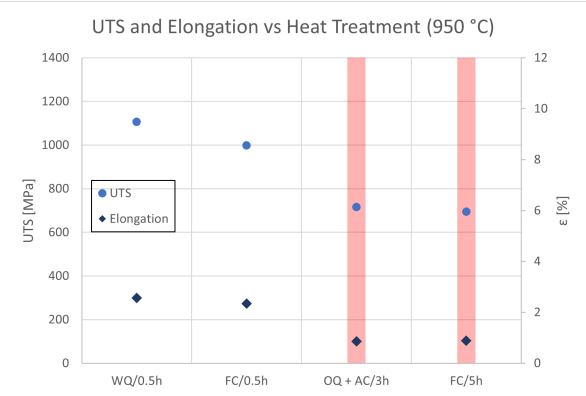

Figure 3: Graphical representation of the UTS and the elongation according to the applied heat treatment, more specifically, at the sitting temperature of 950 °C. The vertical red lines indicate the coupons that fractured prior to reaching the elastic region.

The results obtained go completely against the literature. According to Su et al. [9] where they perform very similar heat treatments, the coupons treated at 950 °C perform at a similar range as the coupons treated at 850 °C: UTS $>$ 1000 MPa, YS $>$ 900 MPa and $\varepsilon > 8$ %. While the parts treated for 30 minutes have UTS and YS values that fall within the target range, these still have very low fracture strain results. The other samples don't even reach the plastic region. The only explanation for these sub-par may come the abnormal defects obtained during manufacturing.

Figure 4: Fracture surface of coupon 15. The photo was taken with a cellphone through a microscope. The red circle highlights a brown spot, which is unexpected in this material.

In figure 4 the fracture surface of coupon 15 is shown. Data for this coupon was not used for the discussion because it slipped twice during the tensile test and the results were not feasible. However, it could be observed that it fractured in the plastic region. There are some differences when compared to P5, namely that the outer area no longer appears to be of ductile nature. Another topic of interest is that there is a brown spot in the center region of the fracture (highlighted with the red circle), the source of which is unidentified.

When comparing to Ropio's results, these cannot be seen as an improvement as the UTS ends up being slightly lower than that of the as-built parts while having the same fracture strain values as the worst ones

3.2.3 Sitting Temperature - 1100 °C

At this sitting temperature, all the coupons fractured before reaching the plastic deformation region. The main takeaway of these tests is the consistent value of the Young's modulus of the parts cooled in the furnace ranging from 105 to 114 GPa. The registered Young's modulus for the oil quenched sample is certainly an outlier given that this value shouldn't be able to deviate this much from the as-built parts.

Even with only 5 tests at this temperature and the fact they fractured early, some conclusions can be taken. The first three samples show that water quenching and furnace cooling yield similar and greater UTS values over oil quenching. The same is not necessarily observed at lower temperatures, like

at 800 °C. Also, from the three samples which were furnace cooled, the most ductile coupon was the one treated for the shortest amount of time. However, the conclusions taken from the specimens that fractured early may not be trustworthy due to variance caused by the defects.

One factor that may have exacerbated the weaknesses of these coupons is the fact that the columnar prior-β grains have been erased from the microstructure. Grain morphology can only be altered at super-transus temperatures ($>$ 1000 °C) but there have been reports of prior-β grains shearing at 950 °C [9]. Treating at these temperatures results in a mix of α and β phases or a new α' phase within the newly formed equiaxed grains. This depends on the cooling rate being that the higher it is, the more it tends to the latter microstructure. This newly formed microstructure favors fatigue type loads as opposed to the elongated prior-β grains which favor creep and tensile loads. [7] Compounded with the preexisting defects, this may have worsened the mechanical properties of the coupons.

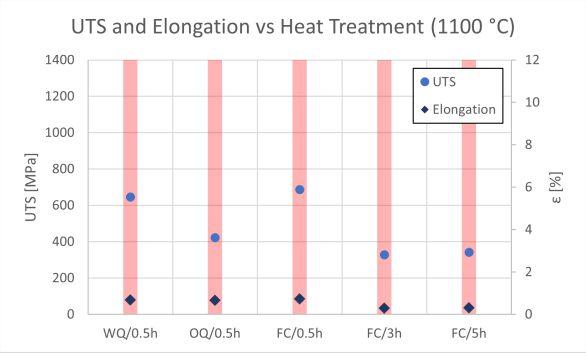

Figure 5: Graphical representation of the UTS and the elongation according to the applied heat treatment, more specifically, at the sitting temperature of 1100 °C. The vertical red lines indicate the coupons that fractured prior to reaching the elastic region.

In figure 6 the fracture surface of a coupon treated at 1100°C is shown. Here the type of fracture is completely different from the previous 2 as it is considerably more brittle. This comes as a result of treating the coupon above the β-transus completely altering the microstructure, as previously mentioned.

3.3. **Overall Analysis**

A full overview of the results can be found in figure 8. From a general perspective, the parts treated at lower temperatures were the ones that performed best as they had less chances of fracturing early. There was also great variability regarding the Young's Modulus. The water quenched samples showed the lowest values, ranging from 88 to 106

Figure 6: Fracture surface of a coupon treated at 1100°C. The photo was taken with a cellphone through a microscope.

GPa, the furnace cooled samples presented results in a more expected range, from 104 to 120 GPa. The highest value was obtained by an oil quenched coupon with 126 GPa. Thermally treated components usually have a Young's modulus up to 10 MPa above or below their as-built counterparts'. [10, 7]

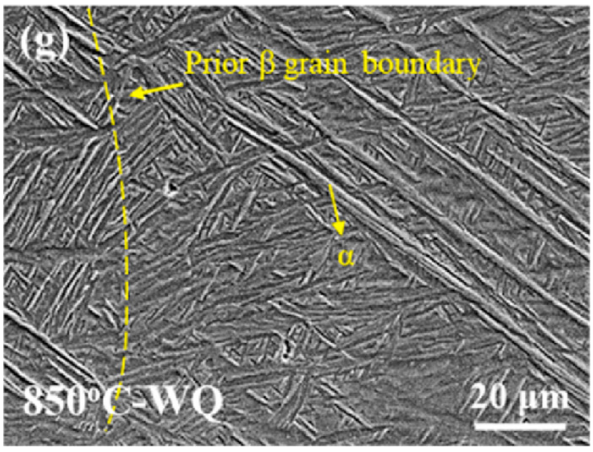

Figure 7: Microstructure of an SLMed sample after being heat treated at 850°C for 2h and being water quenched. [9]

In a study performed by Su et al. [9], they compare the results from heat treating SLMed coupons at 850 °C, 950 °C and 1100 °C (all for 2h) and cooling them down by water quenching, air cooling and furnace cooling. The results obtained were mostly similar (except for the 950 °C treated ones) to those obtained here. The coupons heated at 1100 °C had varying UTS and YS values but the lowest strain (2%) confirming the high brittleness of these specimens and the reason why all of the ones tested here fractured in the elastic region. It's also worth noting that, just like for the water quenched samples, except for the 850 °C one, exhibited the most

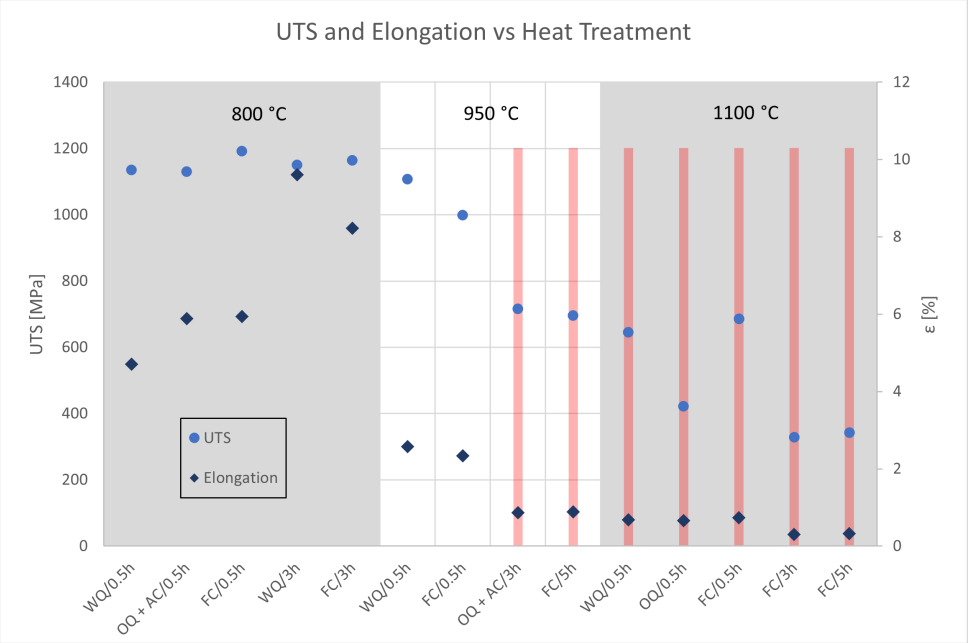

Figure 8: Graphical representation of the UTS and the elongation according to the applied heat treatment, more specifically, the sitting temperature. The vertical red lines indicate the coupons that fractured prior to reaching the elastic region.

brittle characteristics (high UTS and YS, and low strain) in their temperatures. This leads to their final conclusion. The authors claim that the 850 °C + WQ sample resulted in the better combination of mechanical properties, which is in line with the sample with the best mechanical properties (800 °C/3h/WQ). They claim that, upon analyzing the microstructure, the α' phase was transformed into stable α phase while retaining, to a certain extent, the fine and hierarchical grain structure present in as-built parts as seen in figure 7. This allowed for a notable increase in fracture strain in exchange for a slight decrease in UTS and YS.

According to Mur et. al, the acicular α' microstructure present in as-built parts, which is responsible for their more fragile behavior, is completely decomposed when heat treated at temperatures starting at 800 °C. This is, once again, replaced with the more stable phases $\alpha + \beta$. [8] Heat treating at this temperature is also enough to rid the parts of all residual stresses resulting in better mechanical performance. [11] While the second factor is applied to all the heat treated parts, the final microstructure of the part is heavily dependant on all three heat treating parameters depending on whether they were treated at sub-transus or super-transus temperatures. In the end, the most favorable sitting temperature for these coupons was 800 °C, which is one of the most important parameters at sub-transus temperatures. It resulted in the best microstructure, akin to what the previously mentioned study ([9]) reported and presented in figure 7.

3.3.1 Microhardness Testing

For these tests, 5 indentations were performed on the polished surface of each sample with a load of 19.614 N for a duration of 20 seconds. Only one coupon from each combination of parameters was tested plus as-built coupons P4 and P5. The following tables show the results obtained from the hardness testing. Tables 3.3.1 and 6 show the results from the heat treated and the as-built samples respectively. Table 7 shows the average hardness for coupons grouped by an isolated parameter.

The values obtained for the as-built specimens resulted in an average of 433.4 HV, which is high considering the values obtained in the previous dissertation [2] done on the topic (ranging from 350 to 400 HV) but within the expected range found in the literature which specifies values spanning from 300 to 500 HV. [12, 13]

As for the heat treated results, the obtained values ranged from 366 to 671.4 HV. There is a clear correlation between the sitting temperature and the hardness of the specimens. Each average value is separated by roughly 80 HV showing that increasing the temperature results is harder components. The same tendencies can be observed, although to a lesser extent, with the other parameters. Higher resting times also lead to higher hardness values. The different cooling methods only resulted in a

Time [h]	Cooling	Temperature [°C]		
		800	950	1100
0.5	WQ	370.8	409.2	477.8
	OQ	403	499.6	498.8
	OQ + AC	389.8	426.4	529.4
	FC	391.4	415.6	464
3	WQ	366	527.2	583
	OQ	391.8	510.8	623
	OQ + AC	434	439.4	636.2
	FC	373	578	459
5	WQ	464	522.8	581.2
	OQ	379.8	499.8	609
	OQ + AC	450	545.6	671.4
	FC	442.4	488.6	495

Table 5: Surface microhardness [HV] values obtained for the heat treated components.

maximum difference of 50 HV from the lowest and highest averages. Had there been the possibility of testing components that had only been air cooled, it is likely that these would have fallen in between water quenching and furnace cooling as air cooling produces an intermediate cooling rate between the other two methods.

P4	437.2
P5	429.6
Avg.	433.4

Table 6: Surface microhardness [HV] values obtained for the as-built parts.

Temp. [°C]		Time [h]		Cooling	
800	404.67	**0.5**	439.65	**FC**	456.33
950	488.58	**3**	493.45	**WQ**	478
1100	552.32	**5**	512.47	**OQ**	490.62
				AC*	502.47

Table 7: Average microhardness [HV] values for coupons treated with a certain parameter. * OQ+AC

Figure 9 shows the relation between the hardness values and the strain fracture values of the tensile tested specimens. This shows an inverse relation between the values, which was to be expected. The higher the strain, the lower the hardness tends to be (the 950°C/WQ/3h coupon is an outlier in this case). It is also worth noting that the coupon designated to be the best due to its tensile properties registered the lowest hardness out of all tests, with a hardness value of 366 HV.

4. Conclusions

These were the conclusions retained from studying the three parameters (resting time, resting temperature and cooling method) of these heat treatments:

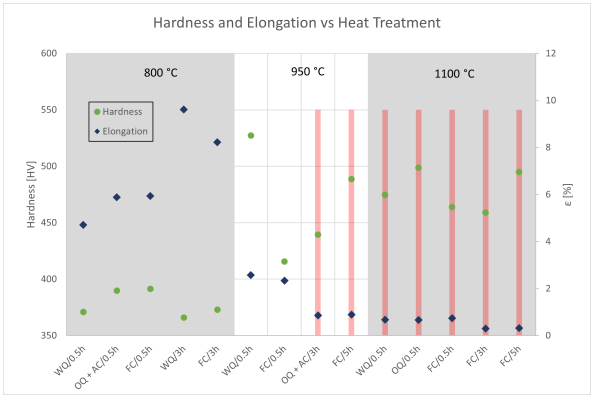

Figure 9: Graphical representation of the hardness and the elongation according to the heat treatment. The vertical red lines indicate the coupons that fractured prior to reaching the elastic region.

- The results obtained emphasize the difficulty in replicating the same results in L-PBF when there is not quality control of every aspect of the printing process. This had consequences in the results of the heat treated samples with many fracturing before reaching the plastic region.

- The used powder is of those aspects and a possible cause for the lackluster results. The information provided by the manufacturer may not be exactly accurate depending on the lot and may yield unpredictable results.

- When performing a first time print of a component, it is always imperative to carefully pick the print parameters in accordance to what is being printed. In this case, coupons were printed vertically with printing parameters that had been optimized for horizontal printing. This is believed to be the reason why most samples underperformed mechanically.

- In addition to the previous point, printing components in layers perpendicular to the direction of the main applied force will generally result in worse mechanical properties as the fracture mechanisms will be different. [6]

- High cooling rates in Ti-6Al-4V components are known to result in an α' martensitic microstructure which turns them brittle. However, when performed after a heat treatment, the lower the sitting temperature, the lower its influence becomes and actually becoming beneficial at a certain point by maintaining a balance of fine grain size and favorable phases.

- The heat treating parameter that affects hardness the most is the resting temperature. The higher it is, the higher the material's hardness will be.

Considering all the identified problems, the fact that the orientation of the coupons was unfavorable both due to non optimized print parameters and bad loading direction, the combination of heat treating parameters that ended up yielding the component with the most favorable assortment of mechanical properties while correcting these issues was the following:

Sitting Temperature [ºC]	800
Sitting Time [h]	0.5
Cooling Method	WQ

Table 8: Heat treating parameters that yielded the best results.

References

[1] 3T-AM. Titanium ti-6al-4v - data sheet.

[2] Beatriz Alexandra Bicho Ropio. Validation of metal additive manufacturing parts. Master's thesis, Universidade de Lisboa - Instituto Superior Técnico, 2018.

[3] Shunyu Liu and Yung C. Shin. Additive manufacturing of ti6al4v alloy: A review. *Materials and Design*, 164:107552, 2019.

[4] Chee Kai Chua, Chee How Wong, and Wai Yee Yeong. *Standards, quality control, and measurement sciences in 3D printing and additive manufacturing*. Elsevier, Academic Press, 2017.

[5] Patrick Hartunian and Mohsen Eshraghi. Effect of build orientation on the microstructure and mechanical properties of selective laser-melted ti-6al-4v alloy. *Journal of Manufacturing and Materials Processing*, 2(4):69, 2018.

[6] M. Simonelli, Y.y. Tse, and C. Tuck. Effect of the build orientation on the mechanical properties and fracture modes of slm ti–6al–4v. *Materials Science and Engineering: A*, 616:1–11, 2014.

[7] T. Vilaro, C. Colin, and J. D. Bartout. As-fabricated and heat-treated microstructures of the ti-6al-4v alloy processed by selective laser melting. *Metallurgical and Materials Transactions A*, 42(10):3190–3199, 2011.

[8] F.x. Gil Mur, D. Rodríguez, and J.a. Planell. Influence of tempering temperature and time on the α'-ti-6al-4v martensite. *Journal of Alloys and Compounds*, 234(2):287–289, 1996.

[9] Chenyu Su, Hanchen Yu, Zemin Wang, Jingjing Yang, and Xiaoyan Zeng. Controlling the tensile and fatigue properties of selective laser melted ti–6al–4v alloy by post treatment. *Journal of Alloys and Compounds*, 857:157552, 2021.

[10] Bey Vrancken, Lore Thijs, Jean-Pierre Kruth, and Jan Van Humbeeck. Heat treatment of ti6al4v produced by selective laser melting: Microstructure and mechanical properties. *Journal of Alloys and Compounds*, 541:177–185, 2012.

[11] S. Leuders, M. Thöne, A. Riemer, T. Niendorf, T. Tröster, H.a. Richard, and H.j. Maier. On the mechanical behaviour of titanium alloy tial6v4 manufactured by selective laser melting: Fatigue resistance and crack growth performance. *International Journal of Fatigue*, 48:300–307, 2013.

[12] J. Tong, C. R. Bowen, J. Persson, and A. Plummer. Mechanical properties of titanium-based ti–6al–4v alloys manufactured by powder bed additive manufacture. *Materials Science and Technology*, 33(2):138–148, 2016.

[13] A. Leicht and E. O. Wennberg. Analyzing the mechanical behavior of additive manufactured ti 6al 4v using digital image correlation. Master's thesis, CHALMERS UNIVERSITY OF TECHNOLOGY, 2015.